Available online at www.sciencedirect.com
ScienceDirect
International Journal of Thermal Sciences 47 (2008) 84–92
International Journal of Thermal Sciences
www.elsevier.com/locate/ijts

Interaction of Lewis number and heat loss effects for a laminar premixed flame propagating in a channel

Subhadeep Chakraborty, Achintya Mukhopadhyay *, Swarnendu Sen

Department of Mechanical Engineering, Jadavpur University, Kolkata 700 032, India

Received 6 July 2006; received in revised form 31 January 2007; accepted 31 January 2007

Available online 26 March 2007

Abstract

A thermo-diffusive model has been used to investigate the interaction of non-unity Lewis number and heat loss for laminar premixed flames propagating in a channel. A coordinate system moving with the flame has been used to immobilize the flame within the computational domain. At Lewis numbers significantly below unity in presence of high heat loss, tip opening near the centerline and dead space near the wall are simultaneously observed, that gives rise to a multicellular flame with "funnel-like" shape. At low Lewis numbers for fluid flow opposing the flame motion, increase in heat loss leads to a transition from inverted "mushroom" to "funnel-shaped" flame. The heat loss has a stronger effect for fluid flows opposing the flame motion than for fluid flows aiding the flame motion. For Lewis numbers above unity, the dependence of reaction rate on Lewis number gets reversed as heat loss increases from zero to a finite value.

Keywords: Flame propagation; Channel; Lewis number; Heat loss; Thermodiffusive model

1. Introduction

Flame propagation in ducts and channels is important for identifying the criteria of flashback in ducts and safety applications in power generation, mining and petro-chemical industries. The problem is also relevant for combustion of gas flowing into the crevice volumes of internal combustion engines [1]. The gas flowing into such small volumes between the piston and the cylinder wall can cool sufficiently by heat loss to the ambient to prevent combustion of the entrapped fuel. This unburned fuel is a major source of unburned hydrocarbon (UHC) emission in internal combustion engines [2]. This geometry has been investigated widely, as is evident from reviews by Williams [3] and Jarosinski [4]. Interest in laminar flame propagation in channels has received renewed attention with the increasing popularization of microscale and mesoscale burners.

Daou and Matalon [5] investigated flame propagation in adiabatic channels in presence of Poiseuille flow, aiding and opposing the propagation of the flame. They adopted a constant density (thermo-diffusive) model. The equations were solved both using an asymptotic method and numerically for unity Lewis number. The critical fluid velocity for flashback was obtained. Subsequently, Daou and Matalon [1] included the effect of heat loss from the walls in terms of a convective heat transfer coefficient but limited their analysis to unity Lewis number. The study focused on the influence of the flow strength, heat loss intensity and channel width on the overall burning rate. They observed complete and partial extinctions in narrow and wide channels respectively. For narrow channels, excessive heat loss led to total extinction of flame in the channel. In channels of moderate width, on the other hand, only partial extinction leading to a dead space near the wall was reported due to heat loss from the walls. In the core region, the flame still continued. The flame was more vulnerable to heat loss when the flow was directed from the unburned to the burned gas. Cui et al. [6] investigated the effect of differential diffusion on flame propagation in thick and thin insulated channels. Their results showed that thick flames (or narrow channels) are not significantly affected by the effective Lewis number of the mixture. Under adiabatic wall conditions, flame propagation speed in relatively narrow channels is independent of the flow direction and

* Corresponding author. Fax: +91 33 24146532; tel.: +91 33 24146177.
E-mail address: amukhopadhyay@mech.jdvu.ac.in (A. Mukhopadhyay).

1290-0729/$ – see front matter
doi:10.1016/j.ijthermalsci.2007.01.025

Nomenclature

b	half channel width
B	preexponential factor
Bi	Biot number, hb/k
D	mass diffusivity
E	activation energy
$\mathbf{h}$	convective heat transfer coefficient
$\hat{\mathbf{i}}$	unit vector in x direction
$\mathbf{k}$	thermal conductivity
Le	Lewis number, α/D
S_u^0	speed of unstretched flame
T_a	activation temperature
T_{ad}	adiabatic temperature
T_u	unburnt gas temperature
U	flame speed
U_{max}	maximum gas velocity
U_p	propagation velocity of a freely propagating plane flame
$\mathbf{V}$	gas velocity vector
X	axial coordinate
y_F	fuel mass fraction
$y_{F,u}$	fuel mass fraction at inlet
Y_F	normalized mass fraction
Z	transverse coordinate
Ze	Zeldovich number, $E(T_{ad} - T_u)/RT_{ad}^2$

Greek symbols

α	thermal diffusivity
ε	ratio of channel half-width to the thickness of the flame preheat zone
γ	heat release parameter, $(T_{ad} - T_u)/T_{ad}$
θ	normalized temperature
$\boldsymbol{\omega}$	chemical reaction rate

depends solely upon the Peclet number based on the relative velocity between the flame and the fluid. On the other hand, a thin flame is strongly affected by the flowfield and may develop regions of high local curvature when the Lewis number is significantly different from unity. They reported flame tip opening or dead space near the walls, depending on whether Lewis number is above or below unity and the flame is concave or convex towards the unburned side.

The results of Cui et al. [7] identify a critical Lewis number as the lower bound for the occurrence of a pulsating mode of propagation for two-dimensional flame fronts traveling in a channel. They concluded that in channels of moderate widths premixed flames are likely to propagate steadily. With excessive wall losses, the critical value of Lewis number is reduced significantly so that oscillations are likely to be observed at near-extinction conditions only. However, their study was limited to $Le > 1$ only.

Using a formulation similar to that of Matalon and coworkers [1,5,6], Kurdyumov and Fernandez-Tarrazo [8] investigated the effect of Lewis number on the propagation of premixed flames through a quiescent fluid in narrow ducts with adiabatic or isothermal (cold) walls. They observed, both mushroom and 'funnel like' flames for isothermal cold walls, depending on the Lewis number and duct radius. For low values of Lewis number, the flame acquired a multi-cellular structure at larger values of duct radius, leading to the transition from mushroom shape to 'funnel like' shape. The quenching radius for isothermal (cold) duct walls strongly depended on Lewis number. They further reported that for $Le < 1$, propagation speed of flames was higher than with adiabatic walls for same duct geometry.

Lee and Tsai [9] identified two major flame shapes in channels, mushroom shape (convex towards the direction of propagation at the centreline) and funnel shape (concave towards the direction of propagation at the centerline). They concluded that the former is the preferred shape for isothermal walls while the latter is observed for adiabatic walls. Hackert et al. [10] investigated the effects of thermal boundary conditions on flame shape and quenching for flames both propagating and stabilized in ducts. They observed a transition from mushroom to funnel shape with increase in duct width for both stationary and propagating flames. They further concluded that adiabatic boundary conditions were not very realistic, as even with low heat transfer coefficients at the wall, the flame shape resembled that for cold (isothermal) walls. However, both these works limited themselves to unity Lewis number effects. Very recently, Michaelis and Rogg [11] solved Navier–Stokes and scalar transport equations to simulate propagation of laminar ozone and hydrogen-air flames in channels. They obtained both mushroom (referred to as meniscus flames) and tulip flames, depending on whether the wall was adiabatic or isothermal. For hydrogen-air flames at lean equivalence ratios, they further obtained tip openings. However, their analysis was limited to flame propagation in quiescent mixtures. Moreover, their analysis did not explicitly bring out the interaction of differential diffusion and heat loss on flame propagation.

None of the above works except Cui et al. [7] considered the combined effects of wall heat loss and non-unity Lewis number on flame propagation in presence of a flow. Moreover, the analysis of Cui et al. [7] was limited for the studies at Lewis number more than unity. However, we expect significant difference in flame behaviour which depends on flame shape for Lewis number less than and more than unity [6]. The motivation of the present work is to study the flame behaviour for both the ranges of Lewis number. Specifically we shall focus on the effects of flame shape and wall heat loss over the entire range of Lewis numbers, which covers a wide range of fuels and stoichiometric ratios. We have also investigated the effect of Lewis number, heat loss and flow velocity on the flame structure, on which information are not readily available in the existing literature.

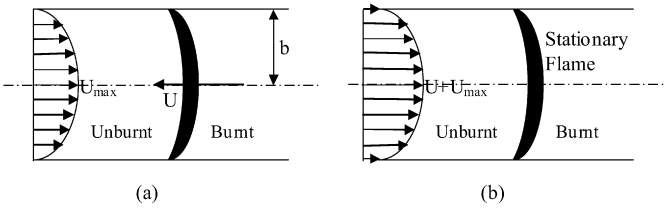

Fig. 1. Schematic of the configuration investigated in (a) laboratory coordinates, (b) moving reference system.

2. Formulation

Flow of a combustible gas mixture in a channel of width $2b$ is modeled. Following [1,5–8], a "thermal diffusive" or constant density model has been used to isolate the effects of the flame on the flow field. A Poiseuille flow has been assumed in the channel using the following velocity distribution.

$$\mathbf{V} = U_{\max}\left(1 - Z^2\right)\hat{\mathbf{i}} \tag{1}$$

The flame propagates with a velocity U in the negative x-direction as shown in Fig. 1(a). Using a reference frame, attached to the flame, the gas velocity field is given by $\{U + U_{\max}(1 - Z^2)\}\hat{\mathbf{i}}$ as shown in Fig. 1(b). The flow can both aid and oppose the flame propagation, depending on whether $U_{\max}$ is negative or positive. Assuming a quasisteady process with respect to a reference frame, moving with the flame, the governing equations are expressed in dimensionless form as

$$\varepsilon\frac{\partial}{\partial X}\left[\left\{U + U_{\max}\left(1 - Z^2\right)\right\}\theta\right] = \frac{\partial^2\theta}{\partial X^2} + \frac{\partial^2\theta}{\partial Z^2} + \omega \tag{2}$$

$$\varepsilon\frac{\partial}{\partial X}\left[\left\{U + U_{\max}\left(1 - Z^2\right)\right\}Y_{\mathrm{F}}\right] = \frac{1}{Le}\left[\frac{\partial^2 Y_{\mathrm{F}}}{\partial X^2} + \frac{\partial^2 Y_{\mathrm{F}}}{\partial Z^2}\right] - \omega \tag{3}$$

The chemical reaction is described by a single step Arrhenius chemistry $\omega = \rho y_{\mathrm{F}} B\exp(-E/RT)$. The chemical reaction is expressed in dimensionless form as

$$\omega = \frac{\varepsilon^2}{U_{\mathrm{p}}^2}\frac{Ze^2}{2Le}Y_{\mathrm{F}}\exp\left[\frac{Ze(\theta - 1)}{1 + \gamma(\theta - 1)}\right] \tag{4}$$

In normalizing the equations, all lengths are scaled with the channel half-width, b and all velocities with the adiabatic planar (unstretched) burning velocity, S_{u}^0. This velocity corresponds to the propagation of an unrestrained planar flame through a quiescent mixture. The normalized temperature and fuel mass fraction are defined as

$$\theta = \frac{T - T_{\mathrm{u}}}{T_{\mathrm{ad}} - T_{\mathrm{u}}} \quad \text{and} \quad Y_{\mathrm{F}} = \frac{y_{\mathrm{F}}}{y_{\mathrm{F,u}}} \tag{5a}$$

Eqs. (1)–(4) also involve the dimensionless quantities, Zeldovich number (Ze), Lewis number (Le), heat release parameter (γ) and the ratio of channel half-width to the thickness of the flame preheat zone (ε), which are defined as follows.

$$Ze = \frac{T_{\mathrm{a}}(T_{\mathrm{ad}} - T_{\mathrm{u}})}{T_{\mathrm{ad}}^2}; \qquad \gamma = \frac{T_{\mathrm{ad}} - T_{\mathrm{u}}}{T_{\mathrm{ad}}}$$

$$Le = \frac{\alpha}{D}; \qquad \varepsilon = \frac{b}{\alpha/S_{\mathrm{u}}^0} \tag{5b}$$

The subscripts a, u and ad refer to activation, unburned and adiabatic temperatures respectively. The terms α and D refer to thermal and mass diffusivities respectively. In the above equation, U_{p} is the propagation velocity of a freely propagating plane flame, defined as $U_{\mathrm{p}} = S_{\mathrm{u}}^0/S_{\mathrm{u},\infty}^0$. The term $S_{\mathrm{u},\infty}^0$ refers to the asymptotic value of the adiabatic planar burning velocity in the limit of large Zeldovich number ($Ze \gg 1$) expressed as

$$S_{\mathrm{u},\infty}^0 = \sqrt{2B\,Le\,Ze^{-2}\alpha}\exp(-T_{\mathrm{a}}/2T_{\mathrm{ad}}) \tag{6}$$

Here B is the preexponential factor. The nondimensional burning velocity U_{p} is given by the solution of the following one-dimensional system of equations.

$$U_{\mathrm{p}}\frac{\partial\theta}{\partial X} = \frac{\partial^2\theta}{\partial X^2} + \frac{Ze^2}{2Le}Y_{\mathrm{F}}\exp\left[\frac{Ze(\theta - 1)}{1 + \gamma(\theta - 1)}\right] \tag{7a}$$

$$U_{\mathrm{p}}\frac{\partial Y_{\mathrm{F}}}{\partial X} = \frac{1}{Le}\frac{\partial^2 Y_{\mathrm{F}}}{\partial X^2} - \frac{Ze^2}{2Le}Y_{\mathrm{F}}\exp\left[\frac{Ze(\theta - 1)}{1 + \gamma(\theta - 1)}\right] \tag{7b}$$

with $\theta = 1 - Y_{\mathrm{f}} = 0$ and 1 as $X \to -\infty$ and ∞ respectively.

The boundary conditions for the channel are as follows.

$$X \to -\infty\text{: } \theta = 1 - Y_{\mathrm{F}} = 0 \text{ (inlet)} \tag{8}$$

$$X \to \infty\text{: } \frac{\partial\theta}{\partial X} = \frac{\partial Y_{\mathrm{F}}}{\partial X} = 0 \text{ (exit)} \tag{9}$$

$$Z = 0\text{: } \frac{\partial\theta}{\partial Z} = \frac{\partial Y_{\mathrm{F}}}{\partial Z} = 0 \text{ (symmetry)} \tag{10}$$

The heat loss from the wall is specified in terms of a convective heat transfer coefficient, h. Hence, at the wall, the following boundary conditions are applied.

$$Z = 1\text{: } \frac{\partial\theta}{\partial Z} + Bi\,\theta = \frac{\partial Y_{\mathrm{F}}}{\partial Z} = 0 \tag{11}$$

The dimensionless heat transfer coefficient (Biot number), Bi is defined as $Bi = hb/k$, where k is the thermal conductivity of the fluid.

3. Numerical procedure

The equations were solved using a pseudo-transient method by adding a transient term to the transport equations. Eqs. (1)–(4), subject to boundary conditions (8)–(11) were discretized using a second order accurate three point finite volume method. A time marching explicit procedure using first order predictor-corrector method [8] was adopted. The final solution was obtained as a steady state solution with respect to a coordinate system moving with a velocity U. The velocity U was determined iteratively to fix the flame near the center of the computational domain. The iteration involved satisfying the integral form of the species equation.

$$\left(U + \frac{2}{3}U_{\max}\right)\left(1 - \int_{Z=0}^{1} Y_{\mathrm{F}}|_{X\to\infty}\,\mathrm{d}Z\right) = -\int_{X\to-\infty}^{\infty}\int_{Z=0}^{1}\omega\,\mathrm{d}Z\,\mathrm{d}X \tag{12}$$

The solution is initialized by assuming a one-dimensional (axially varying) profile for both temperature and fuel mass fraction. The temperature increased linearly from 0 to 1 and the fuel mass fraction decreased linearly from 1 to 0 in the domain $-0.5 \leqslant X \leqslant 0.5$.

4. Results and discussions

The results presented in this section correspond to $Ze = 8$, $\gamma = 0.85$ and $\varepsilon = 6$ for various values of Le and Bi for $U_{\max} = \pm 1$. Before presenting the results for parametric variations in the above parameters, the sensitivity of the results to grid size are determined.

4.1. Sensitivity to grid size

Eqs. (1)–(4) were discretized on a uniform grid. Fig. 2 shows the results for $Le = 0.5$, $Bi = 0$ and $U_{\max} = 1$ using a relatively coarse grid size of 301×101 and a more refined grid structure of 601×201 for a domain extending in the axial direction from -2 to 4. Extensive numerical experiments with different positions of inlet and exit boundaries revealed that the above size was sufficiently large that the location of the inlet and the exit boundaries did not affect the results. As we observe from the figure, both the reaction rate contours (solid lines) and the isotherms, measures of the accuracy of simulating the transport processes in the reaction and preheat zones respectively, are practically indistinguishable for the two grids. Hence, we adopt the grid size of 301×101 for our simulations.

4.2. Flame shapes

Fig. 3 shows the reaction rate contours for different values of Biot numbers at $Le = 0.5$ for $U_{\max} = 1.0$. Consistent with the

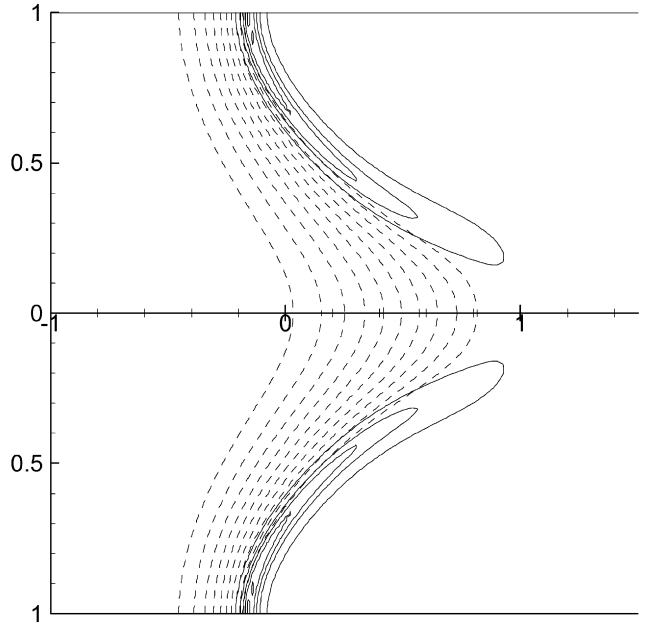

Fig. 2. Comparison of isotherms and reaction rate contours for $Le = 0.5$, $Bi = 0$ and $U_{\max} = 1$ using 301×101 (top) and 601×201 (bottom) grids.

observations of Cui et al. [6], for adiabatic walls ($Bi = 0$) and low heat losses ($Bi = 0.5$) flame tip opening is observed near the centerline while burning is intensified near the wall. The flame extinction near the axis is a characteristic feature of concave (towards the reactant side) flames with $Le < 1$ for which the defocusing of reactants dominates over the focusing of heat. However, for $Bi = 0.5$, the zone of maximum reaction rate shifts slightly away from the wall. As Biot number increases further ($Bi = 1.0$), burning becomes weakened at the wall as well, owing to increased heat loss. Consequently, the peak reaction zone shifts away from the wall. Simultaneously, the leading edge of the flame shifts from the wall to the interior of the channel. As the heat loss increases, the curvature of the flame, which at the wall is convex towards the unburnt mixture, decreases and the flame becomes flatter ($Bi = 0.5$). With further increase in heat loss, there is an inversion of the flame, giving a small region (concave towards the unburnt side) of weak combustion near the wall ($Bi = 1.0$). The shifting of the leading edge of the flame from the wall to the interior gives a multi-cellular flame structure that has a "funnel like" shape. Possibly this is a result of local quenching near the walls, the mixture finds itself ahead of the nearly flat flame front, and because of the high temperature, reaction occurs along a segment which is locally almost parallel to the walls. Lee and Tsai [9] observed that "funnel like" and mushroom flames are the preferred flame shapes for channels with adiabatic and isothermal (cooled) walls respectively. Hackert et al. [10] also observed transition of flame shapes from mushroom to "funnel like" shape in presence of heat loss as the channel width is increased. Kurdyumov and Fernandez-Tarrazo [8] observed a transition to "funnel like" flame structures as the channel width increased at low Lewis numbers and isothermal (cold) duct walls. The transition from an inverted "mushroom" flame to "funnel like" flame due to increased heat loss has not been reported earlier, to the authors' knowledge. The earlier references to evolution of such flames [8,10] were a consequence of increase in channel width. As the Biot number increases even further ($Bi = 5.0$), tip opening and dead space near the wall are simultaneously observed.

Fig. 3 also shows the corresponding isotherms. In each of the cases, the maximum temperature exceeds the adiabatic flame temperature. This can be attributed to the curvature of the flame at the leading edge. The curvature of the flame near the wall is primarily caused by the heat loss. Due to the curvature of the flame (concave towards the burned side) at the location of the maximum heat release, there is a focusing of energy beyond the flame that leads to a local increase of temperature beyond the adiabatic flame temperature, in spite of increasing heat loss. A similar phenomenon has also been observed in [8]. A comparison of the isotherms for $Bi = 0$ and $Bi = 0.5$ reveals that there is a distinct difference in the temperature pattern, although the flame contours in the two cases are very similar qualitatively. This is because of the fact that the major heat loss occurs in the post-flame region. As explained by Law and Sung [12], heat loss downstream of the flame affects the flame only indirectly through modification of temperature gradient at the flame surface. In presence of heat loss, a significant cooling is observed along the wall. As the heat loss increases, the region of

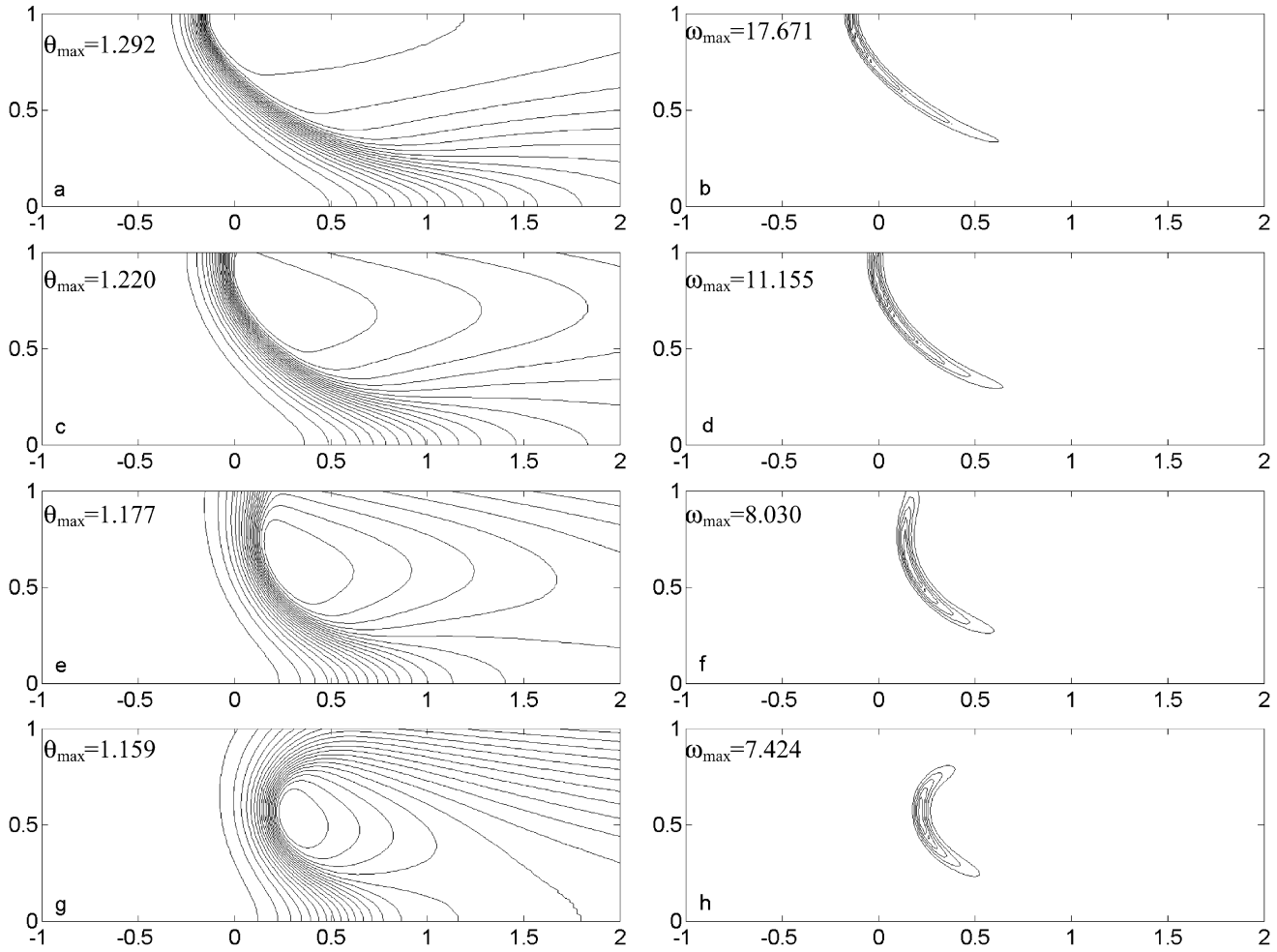

Fig. 3. Isotherms (left) and reaction rate contours (right) for different Biot numbers at $Le = 0.25$ and $U_{\max} = 1.0$. a,b: $Bi = 0$; c,d: $Bi = 0.5$; e,f: $Bi = 1.0$; g,h: $Bi = 5.0$.

maximum burned gas temperature decreases to a small cell. At a high value of Biot number ($Bi = 5$), expectedly, the channel wall becomes nearly isothermal, approaching the temperature of the cold unburned gas.

The interaction of Biot number and Lewis number can be analyzed by comparing the effect of Biot number on flame shapes at different Lewis numbers. Fig. 4 shows the temperature and reaction rate contours for different values of Biot numbers at $Le = 0.5$ and 0.75 for $U_{\max} = 1.0$. A comparison with Fig. 3 reveals that the flame shapes are similar for $Le = 0.25$ and 0.5. However, the flame broadens considerably at $Le = 0.5$ in comparison with that for $Le = 0.25$. The change in flame width corroborates the fact that the reaction is more intense at lower Lewis number due to curvature effects. At $Bi = 0.5$, tip opening is not observed for $Le = 0.75$ and the tip opening increases as Lewis number decreases. As noted by previous authors [6,12, 13], concave flame tips undergo flame tip opening for $Le < 1$ and the effect becomes more prominent as the Lewis number changes significantly from unity. The flame curvature also increases with decrease in Lewis number. A decrease in Lewis number tends to push the location of peak reaction rate towards the wall for $U_{\max} > 1$ while increase in heat loss will cause a shift in this location towards the core. This is evident from the observation that as Lewis number decreases for a given Biot number ($Bi = 0.5$), the zone of maximum chemical reaction moves towards the wall. The increase in flame curvature at lower Lewis number causes a progressive increase in the maximum temperature of burned gas beyond the adiabatic flame temperature and absence of high temperature 'cells' at $Le = 0.75$. At higher rates of heat loss ($Bi = 1$), the effect of Lewis number is more pronounced. The flame tip opening, observed at $Le = 0.25$, is not found at $Le = 0.5$. On the other hand, at $Le = 0.75$, tip extinction is completely absent. In fact, the reaction rate appears stronger near the centerline. The flame is much broader and appears close to extinction and exhibits a dead space near the wall. Evidently, for this set of parameter values ($Le = 0.75$ and $Bi = 1$), the effect of heat loss dominates over that of Lewis number. As in the case of $Bi = 0.5$, the curvature increases and the flame width decreases with decrease in Lewis number. The isotherms also reveal a different pattern at $Le = 0.75$, compared to those at $Le = 0.25$ and 0.5. Expectedly, the value of maximum temperature decreases with increase in Lewis number.

Fig. 5 demonstrates the effect of heat loss on for $U_{\max} = -1$ and $Le = 0.5$. In this case, the leading edge of the flame is on the axis and at the leading edge, the flame is convex towards the

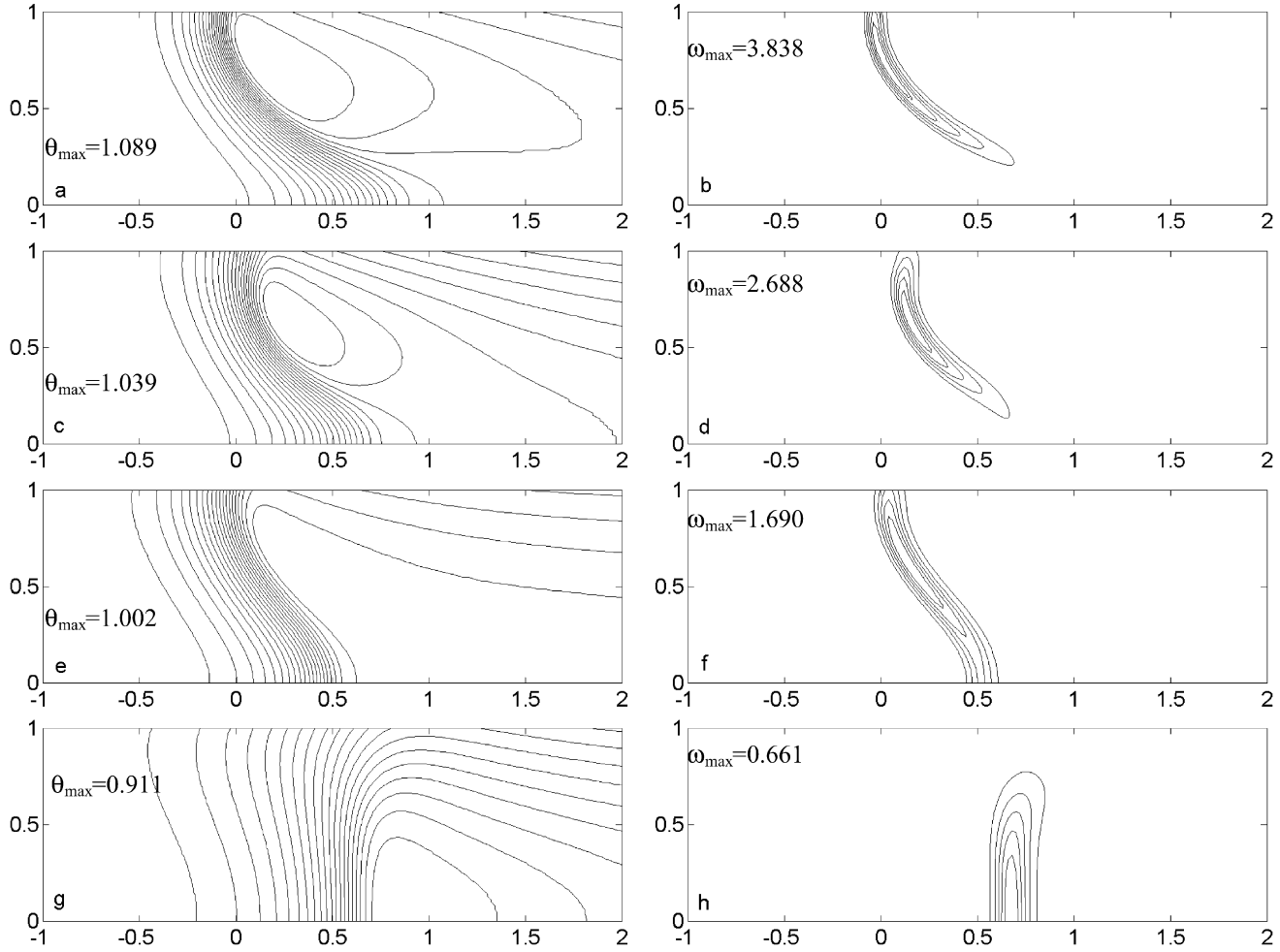

Fig. 4. Isotherms (left) and reaction rate contours (right) for different Biot numbers and Lewis numbers at $U_{\max} = 1.0$. a,b: $Le = 0.5$, $Bi = 0.5$; c,d: $Le = 0.5$, $Bi = 1.0$; e,f: $Le = 0.75$, $Bi = 0.5$; g,h: $Le = 0.75$, $Bi = 1.0$.

unburned side. As reported by Cui et al. [6], for adiabatic walls, a dead space develops near the wall and reaction is strongest near the axis. As the heat loss increases, the flame curvature increases. However, the effect of increased heat loss on the flame shape is much less pronounced than the case of $U_{\max} = 1$. In this case, the flame is convex at the axis and this curvature is caused primarily due to heat loss. This curvature tends to promote fuel consumption for $Le < 1$. However, this is counterbalanced by the dissipative action of increased heat loss, making the flame less sensitive to variations in Biot number. As in the previous case, here also, the curvature causes an increase in the burned gas temperature beyond the adiabatic flame temperature.

The effect of Biot number on flame shape for $Le > 1$ is depicted in Fig. 6. The results are presented for $U_{\max} = -1$. For this configuration, the flame is concave at the wall, which is the trailing edge of the flame. Since $Le > 1$, focusing of heat dominates over the defocusing of the reactants at the concave region, strengthening the flame at that region. On the other hand, at the centerline, opposite curvature leads to weakening of the flame. For $Bi = 0$, as the Lewis number increases, the reaction rate becomes more intensified near the wall because of preferential diffusion effects. A comparison with Figs. 2 and 3 clearly reveal the similarity of the flame shapes for $Le > 1$ and $U_{\max} = -1$ (convex at the centerline) with that for $Le < 1$ and $U_{\max} = 1$ (concave at the centerline) at $Bi = 0$. As Biot number increases, the effect of heat loss dominates and consequently, the effect of stretch and preferential diffusion becomes less pronounced. Further for $\mathbf{U}_{\max} = -1$, as Lewis number increases, the reaction tends to become weaker near the axis and intensified near the wall. However, increase in Biot number affects the wall region most strongly and predominates over the diffusion-induced intensification of reaction at the wall. Consequently, at higher Biot number, increasing Lewis number primarily weakens the reaction near the centerline. Thus for $Bi = 0.5$ and 1, both the peak reaction rate and the flame shape suggest weaker reactions for $Le = 2$ compared to that for $Le = 1.5$. This is in contrast with the situation for $Bi = 0$, where the preferential diffusion effect alone prevails, making the flame stronger at $Le = 2$.

4.3. Flame structure

Figs. 7, 8 depict the effects of Lewis number and heat loss on the internal structure of the flame. For investigating the flame structure, the temperature and species distributions are considered across the flame at the transverse position where reaction

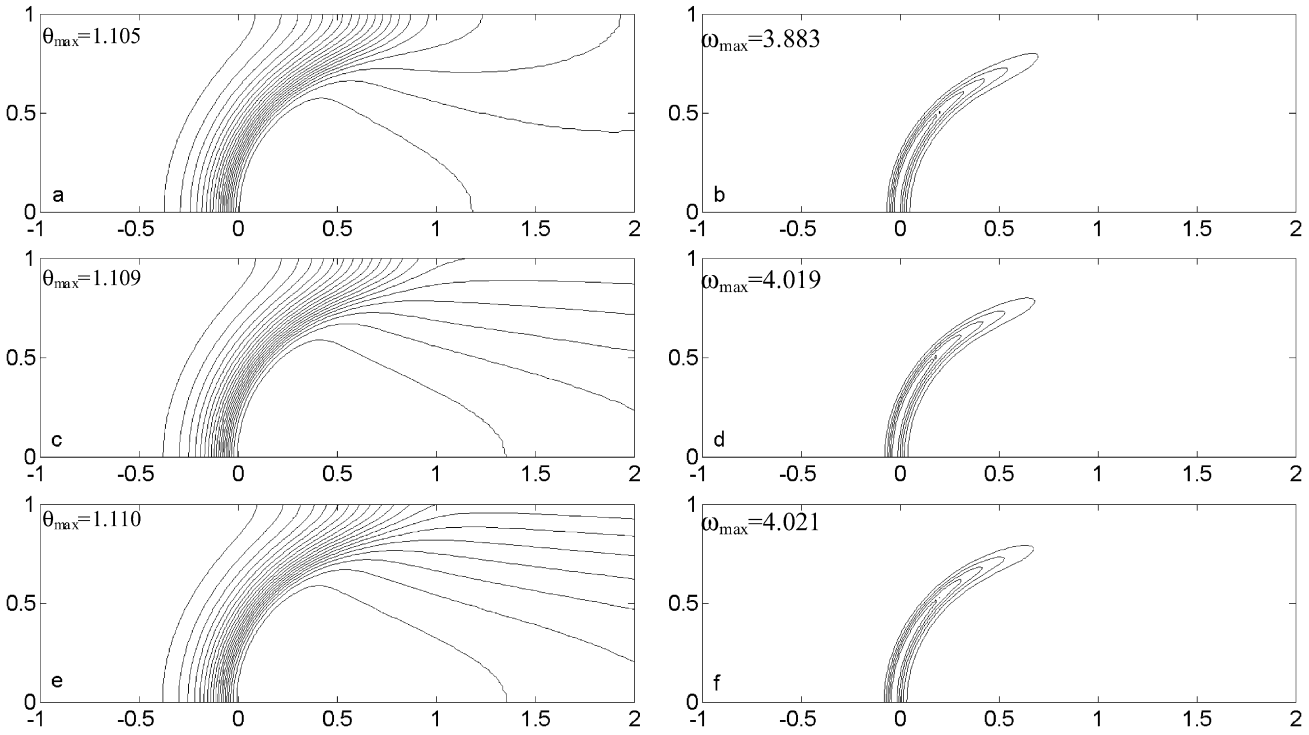

Fig. 5. Isotherms (left) and reaction rate contours (right) for different Biot numbers at $Le = 0.5$ and $U_{\max} = -1.0$. a,b: $Bi = 0$; c,d: $Bi = 0.5$; e,f: $Bi = 1.0$.

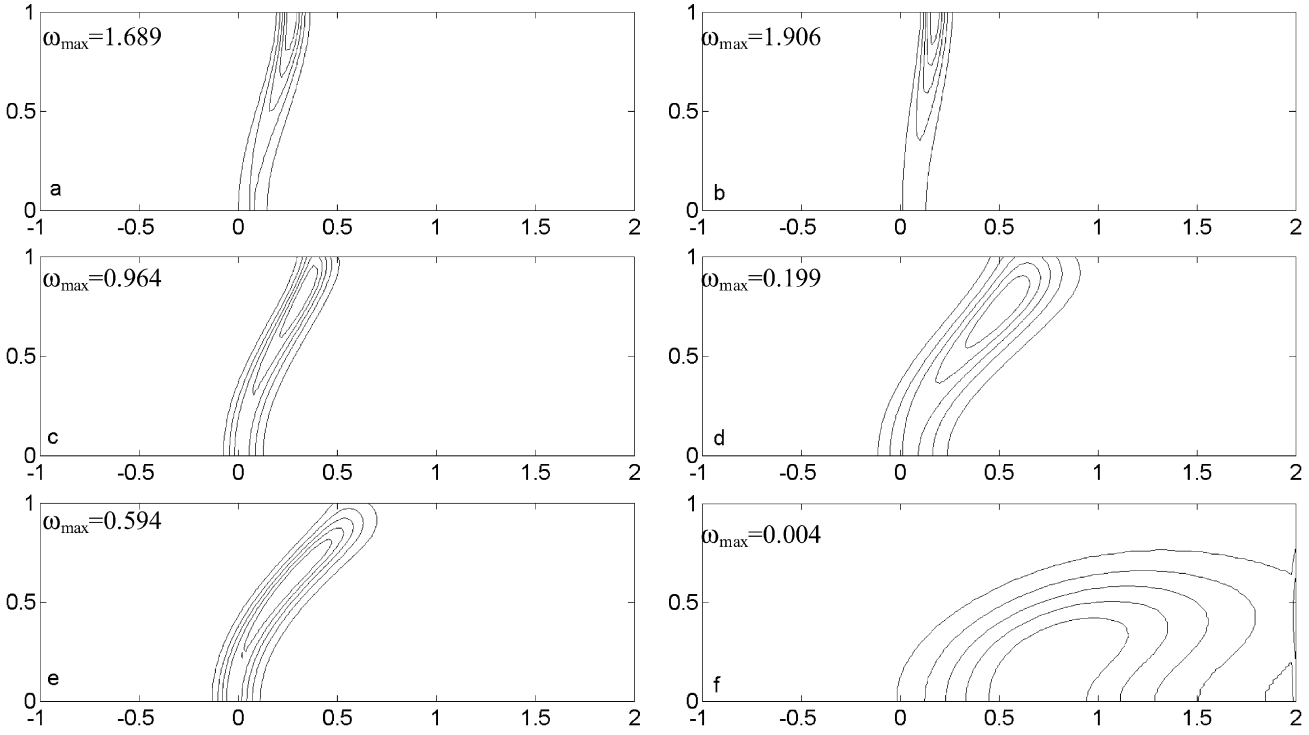

Fig. 6. Reaction rate contours for $Le = 1.5$ (left) and $Le = 2.0$ (right) for different Biot numbers at $U_{\max} = -1.0$. a,b: $Bi = 0$; c,d: $Bi = 0.5$; e,f: $Bi = 1.0$.

rate is maximum. In each of the figures, the flame is shifted so that the location of the peak reaction coincides with the origin. Fig. 7 demonstrates the effect of Biot number on the flame structure for $Le = 0.25$ and $U_{\max} = 1$. For different Biot numbers, the major difference in the temperature profiles is downstream of the reaction zone. As Biot number increases, the heat loss through the wall increases. Since the temperature difference between the gases and the ambient is very small in the upstream zone and the preheat zone occupies a very small fraction of the axial extent of the computation domain, the bulk of

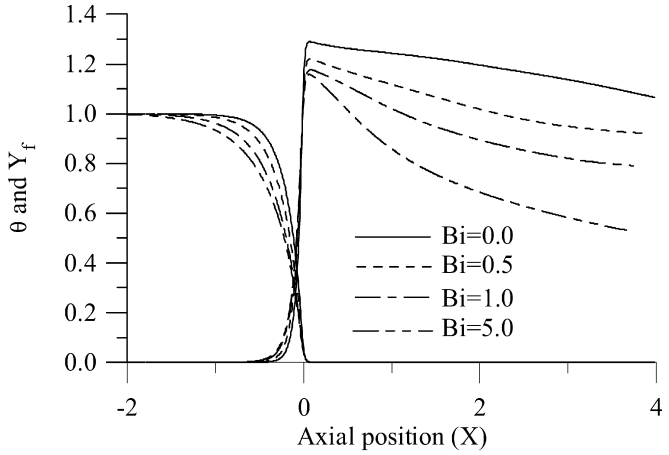

Fig. 7. Axial variation of temperature and fuel concentration across the flame for different Biot numbers at $U_{max} = 1.0$ and $Le = 0.25$.

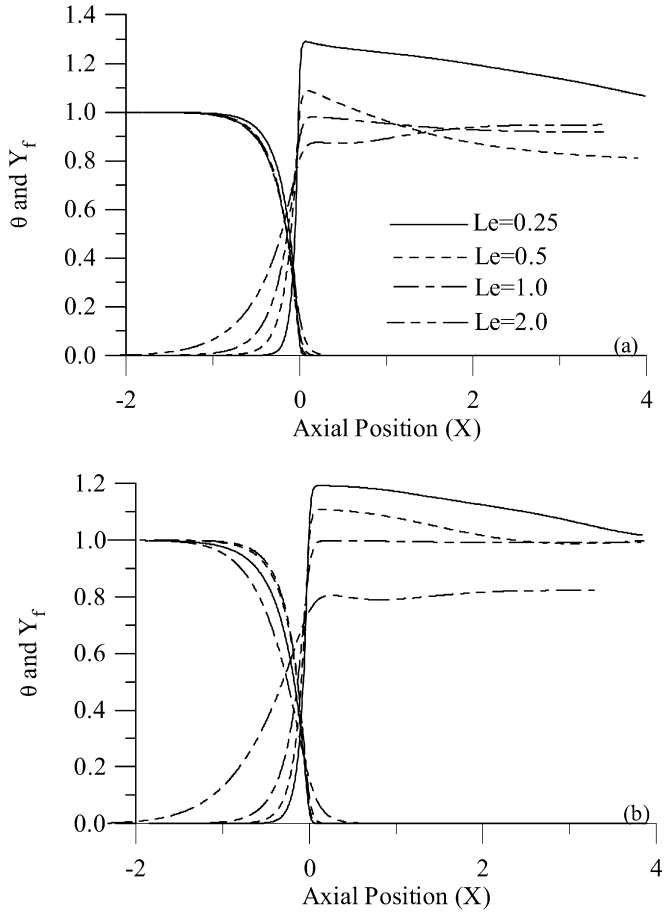

Fig. 8. Axial variation of temperature and fuel concentration across the flame for different Lewis numbers at $Bi = 0.5$ and (a) $U_{max} = 1.0$ and (b) $U_{max} = -1.0$.

the heat losses take place from the burned gases. Consequently, the temperature profile is also very similar in each case, upstream of the flame. However, the fuel concentration profiles reveal significant sensitivity to heat loss. With increasing heat loss, the length of the diffusion zone for the species concentration increases. As heat loss increases, the convex curvature of the flame increases at the region of maximum reaction. Increasing curvature in the convex region implies a stronger focusing effect for the reactants at $Le < 1$. This leads to a higher rate of fuel consumption at the flame. This is reflected through a more pronounced mass diffusion, leading to broadening of the diffusion zone. Such broadening of the diffusion zone, induced by flame curvature, has also been reported by Poinsot et al. [14] in the context of Bunsen flame tips.

Fig. 8 shows the temperature and species profiles within the flame for different Lewis numbers at a given Biot number ($Bi = 0.5$) for both aiding and opposing flows. For $U_{max} > 0$, the fuel concentration profiles show similar qualitative and quantitative trends at different Lewis numbers, while temperature profiles show significant variations both before and after the flame. The temperature profile for $Le = 2$ shows an increase in temperature beyond the flame. For both aiding ($U_{max} = -1$) and opposing ($U_{max} = 1$) flows, the flame is convex (towards the unburned side). This implies that there is a focusing of energy beyond the flame. Similar factors are responsible for the flame temperature exceeding the adiabatic flame temperature for $Le < 1$. In this case, however, in the preheat zone, the defocusing of energy dominates over focusing of the reactants, causing weak reaction in the flame zone. Consequently, the temperature at the reaction zone is substantially below the adiabatic value. Subsequent temperature profile is determined by two competing factors. On one hand, heat loss from the flame tends to cool the gas downstream. On the other hand, diffusion of heat focuses the energy, promoting an increase downstream. As Lewis number increases, weaker reaction leads to a lower flame temperature. This implies a lower heat loss to the ambient for a given Biot number. At the same time, higher Lewis number implies a stronger effect of diffusion. Thus with increasing Lewis number, the second effect tends to dominate over the first. This is revealed in the temperature profiles. For $Le < 1$, the gas temperature decreases downstream while for $Le = 1$, the value remains close to the adiabatic value throughout. The integral analysis of Sun et al. [15] reveals that the difference of burned gas temperature from adiabatic flame temperatures for flames at low stretch rates and negligible heat loss is proportional to $(Le^{-1} - 1)$. Daou and Matalon [1] also report maximum temperatures close to unity for low Biot numbers.

5. Conclusions

The interaction of preferential diffusion and heat loss for laminar premixed flames propagating in a channel has been investigated using a thermal diffusive (constant density) model. A Galilean transformation has been used to immobilize the flame within the computational domain. The propagation speed of the flame is determined from an integral balance of the species equation over the entire domain. A pseudo-transient predictor-corrector algorithm that is first order accurate in time and second order accurate in space has been employed for the solution of the conservation equations. For Lewis numbers much less than unity, and high heat loss, transition from an inverted mushroom to funnel-shaped flame has been observed. This is caused by simultaneous existence of tip opening near

the centerline and dead space near the wall. The effect of heat loss from the flame is more pronounced for fluid flow opposing the flame motion than for flow aiding the flame motion. For $Le > 1$ and $U_{\max} = -1$, the dependence of the reaction rate on Lewis number gets reversed as Biot number increases. Future plan of work includes experimental validation of the results by investigating the propagation and dynamics of flame in a channel using different reactant mixtures and equivalence ratios to simulate different Lewis numbers. The flame structure and propagation speed can be investigated using direct images from CCD camera and high-speed camera respectively.

References

[1] J. Daou, M. Matalon, Influence of conductive heat-losses on the propagation of premixed flames in channels, Combust. Flame 128 (2002) 321–339.
[2] J.B. Heywood, Internal Combustion Engine Fundamentals, McGraw-Hill Publishing Company, New York, 1988.
[3] F.A. Williams, Combustion Theory, second ed., The Benjamin/Cummings Publishing Company, Menlo Park, 1985.
[4] J. Jarosinski, A survey of recent studies on flame extinction, Prog. Energy Combust. Sci. 12 (1986) 81–116.
[5] J. Daou, M. Matalon, Flame propagation in Poiseuille flow under adiabatic conditions, Combust. Flame 124 (2001) 337–349.
[6] C. Cui, M. Matalon, J. Daou, J. Dold, Effects of differential diffusion on thin and thick flames propagating in channels, Combust. Theory Model. 8 (2004) 41–64.
[7] C. Cui, M. Matalon, T.L. Jackson, Pulsating mode of flame propagation in two-dimensional channels, AIAA J. 43 (2005) 1284–1292.
[8] V.N. Kurdyumov, E. Fernandez-Tarrazo, Lewis number effects on the propagation of premixed laminar flames in narrow open ducts, Combust. Flame 128 (2002) 382–394.
[9] S.T. Lee, H.T. Tsai, Numerical investigation of steady laminar flame propagation in circular tubes, Combust. Flame 99 (1994) 484–490.
[10] C.L. Hackert, J.L. Ellzey, O.A. Ezekoye, Effects of thermal boundary conditions on flame shape and quenching in ducts, Combust. Flame 112 (1998) 73–84.
[11] B. Michaelis, B. Rogg, FEM simulation of laminar flame propagation I: Two-dimensional flames, J. Comput. Phys. 196 (2004) 417–447.
[12] C.K. Law, C.J. Sung, Structure, aerodynamics, and geometry of premixed flamelets, Prog. Energy Combust. Sci. 26 (2000) 459–505.
[13] M. Mizomoto, Y. Asaka, S. Ikai, C.K. Law, Effects of preferential diffusion on burning intensity of curved flames, Proc. Combust. Inst. 20 (1984) (2000) 1933–1939.
[14] T. Poinsot, T. Echekki, M.G. Mungal, A study of the laminar flame tip and implications for premixed turbulent combustion, Combust. Sci. Technol. 81 (1992) 45–73.
[15] C.J. Sun, C.J. Sung, L. He, C.K. Law, Dynamics of weakly stretched flames: quantitative description and extraction of global flame parameters, Combust. Flame 118 (1999) 108–128.